



**HAL**  
open science

# Evaluation of semi-mechanistic models to predict soil to grass transfer factor of $^{137}\text{Cs}$ based on long term observations in French pastures

Khaled Brimo, Laurent Pourcelot, Jean Michel Metivier

## ► To cite this version:

Khaled Brimo, Laurent Pourcelot, Jean Michel Metivier. Evaluation of semi-mechanistic models to predict soil to grass transfer factor of  $^{137}\text{Cs}$  based on long term observations in French pastures. Journal of Environmental Radioactivity, 2020, 227 (106467), pp.106467. 10.1016/j.jenvrad.2020.106467 . hal-03149290

**HAL Id: hal-03149290**

**<https://hal.science/hal-03149290>**

Submitted on 22 Feb 2021

**HAL** is a multi-disciplinary open access archive for the deposit and dissemination of scientific research documents, whether they are published or not. The documents may come from teaching and research institutions in France or abroad, or from public or private research centers.

L'archive ouverte pluridisciplinaire **HAL**, est destinée au dépôt et à la diffusion de documents scientifiques de niveau recherche, publiés ou non, émanant des établissements d'enseignement et de recherche français ou étrangers, des laboratoires publics ou privés.



Distributed under a Creative Commons Attribution - NonCommercial - NoDerivatives 4.0 International License

1 **Evaluation of semi-mechanistic models to predict soil to grass**  
2 **transfer factor of  $^{137}\text{Cs}$  based on long term observations in French**  
3 **pastures**

4 Khaled Brimo<sup>a\*</sup>, Laurent Pourcelot<sup>a</sup>, Jean Michel Métivier<sup>a</sup>, Marc André Gonze<sup>a</sup>

5 <sup>a</sup> Institut de Radioprotection et de Sûreté Nucléaire (IRSN), LEREN, Cadarache, 13115 Saint  
6 Paul lez Durance, France

7 \*Corresponding authors: Khaled BRIMO

8 Tel: + 33 04.42.19.91.09

9 E-mail: [khaledbrimo@gmail.com](mailto:khaledbrimo@gmail.com)

10

11

12

13

14

15

16

17

18

19

20 **Abstract**

21 The aim of this study was to evaluate and improve the accuracy of the semi-mechanistic  
22 models used in regulatory exposure assessment tools, to describe the transfer factors (*TF*) of  
23  $^{137}\text{Cs}$  from pasture soils to grass observed in different grazing areas of France between 2004  
24 and 2017. This involved a preliminary parameterization step of the dynamic factor describing  
25 the ageing of radiocesium in the root zone using a Bayesian approach. A data set with mid-  
26 term (10 years about) and long term (more than 20 years) field and literature data from 4  
27 European countries was used. A double kinetics of the bioavailability decay was evidenced  
28 with two half-life periods equal to  $0.46\pm 0.11$  yr and  $9.57\pm 1.12$  yr for the fast and slow  
29 declining rates respectively. We, then, tested a few existing alternative models proposed in  
30 literature. The comparison with field data showed that these models always underestimated  
31 the observations by one to two orders of magnitude, suggesting that the solid-liquid partition  
32 coefficient (*Kd*) was overestimated by models. The results suggest that semi mechanistic  
33 models might fail in the long-term prediction of the radionuclide transfer from soil-to-plant in  
34 the food chain. They highlight the need to calculate *Kd* using easily exchangeable  $^{137}\text{Cs}$  (i.e.  
35 labile fraction) rather than total soil  $^{137}\text{Cs}$ .

36

37

38 **Keywords:** Cesium 137, Bioavailability, Chernobyl and global fallout, Absalom model,  
39 Parameter estimation, Uncertainty

40

41

42

## 43 **1. Introduction**

44 During the last two decades, numerous radioecological models have been developed to predict  
45 the soil-to-plant transfer of radiocesium ( $^{137}\text{Cs}$ ) in pastures contaminated by atmospheric  
46 fallouts (Absalom et al., 2001; Wright et al., 2003; Yamamura et al., 2018). A better  
47 quantitative understanding of food-chain transfers is of primary importance when assessing  
48 the radiation exposures and doses to man, notably in case of a nuclear accident. Models  
49 essentially differ in the level of complexity adopted in both the conceptual description of the  
50 soil-plant system (e.g. features, events and processes) and the mathematical parameterization  
51 of the biological and physico-chemical mechanisms considered (Almahayni et al., 2019). One  
52 of the simplest approaches is the well-known Transfer Factor approach (IAEA-TECDOC-472,  
53 2010) which fails to explain the observed variability. More elaborated approaches have been  
54 developed which try to explicitly account for the influence of some important environmental  
55 characteristics (e.g. soil properties) through semi-mechanistic parameterizations. Examples of  
56 semi mechanistic approaches are the models published by Absalom et al. (2001), Tarsitano et  
57 al. (2011) and Uematsu et al. (2015) which enable to assess the transfer of cesium based on  
58 some soil properties (e.g. clay content, organic matter content, exchangeable potassium) and  
59 the time elapsed since the initial deposit. These models explicitly take into account the  
60 phenomena associated with the decrease of  $^{137}\text{Cs}$  bioavailability during the years following  
61 the deposition phase by introducing a dynamic factor depending on the time elapsed since the  
62 deposition date. Special attention should be paid to its estimation since its value may  
63 drastically influence the predicted activity in plants.

64 Despite findings indicating that bioavailability of radiocesium in soil decreases with time  
65 (Absalom et al., 1995; Brimo et al., 2019; Smith et al., 1999), these models have been often  
66 developed and tested against data sets mostly limited to laboratory experiments on relatively  
67 short time scales (i.e. from a few days to a few years) .Thus, the validity of these models

68 under real field conditions and on longer time scales (i.e. several decades after an accident) is  
69 highly questionable. Additionally, the uncertainties associated to the model parameters and  
70 their impacts on model predictions have not been addressed in the literature. The main  
71 objective of the present work was to evaluate the performance of these semi-mechanistic  
72 models by comparing the predicted soil-to-pasture vegetation transfer factors with field  
73 observations acquired in French pastures on the long term (i.e. 20 to 30 years after Chernobyl  
74 and 50 years after global fallout). Such an objective also implies to more reliably quantify the  
75 bioavailability decay rates on both mid and long terms after deposition, and their respective  
76 contributions. This was accomplished by calibrating these constants against mid-term (10  
77 years about) and long term (more than 20 years) field and literature data acquired after  
78 Chernobyl accident in several European countries, based on a Bayesian approach.

## 79 **2. Material and methods**

### 80 **2.1. Model descriptions**

81 The simplest approach to quantify the soil-to-grass vegetation transfer of radiocesium in  
82 pastures relies on the use of an aggregated transfer coefficient  $T_{ag}$  (in  $m^2/kg$ ) which quantifies  
83 the activity concentration in grass vegetation in (Bq/kg) normalized by the activity inventory  
84 in soil (in  $Bq/m^2$ ) (IAEA-TECDOC-472, 2010). This definition can also be extended to  
85 cow's milk in the considered ecosystem (i.e. soil-to milk aggregated transfer factor). One  
86 major drawback of this approach is the large spatial variability of  $T_{ag}$  values - even on a small  
87 area - due to the quite inhomogeneous  $^{137}Cs$  deposition patterns. In addition to spatial  
88 variability, a decrease of  $T_{ag}$  values over time was often observed as a result of the decrease of  
89 cesium availability in the root soil due to both its irreversible fixation on soil particles and its  
90 migration down through the soil profile (Albers et al., 2000; IAEA-TECDOC-472, 2010).  
91 These lead thus to a substantial over or underestimate of the predicted risk, and therefore this

92 approach was not used in this work. An alternative approach to quantify the soil-to-grass  
 93 transfer of radiocesium in pastures relies on the use of a soil-to-grass transfer factor  $TF$   
 94 (dimensionless), defined as the ratio between the radioactivity concentration in grass ( $C_V$  in  
 95 Bq/kg<sub>dm</sub> where dm denotes to dry mass) to that in the root soil layer ( $C_S$  in Bq/kg<sub>dm</sub>) (see  
 96 equation (1) below). This approach is only valuable when the contribution of the foliar  
 97 pathway becomes negligible and the uptake by roots is the major process controlling the  
 98 radionuclide activity concentration in grass. It is usually assumed that  $TF$  is constant with  
 99 time, although its value is tabulated for different groups of soils and plants (IAEA-TECDOC-  
 100 472, 2010):

$$TF = \frac{C_V(t)}{C_S(t)} = cte \quad (1)$$

101 Using equation (1), it is possible to predict the radiocesium concentration in grass at any time  
 102 (t) recognizing the tabulated  $TF$  value and the radioactivity concentration in the root layer of  
 103 soil. To refine the approach, Absalom et al. (1999) proposed in their model to partition the  
 104 <sup>137</sup>Cs content in the root layer into two fractions : a non-bioavailable one that evolves over  
 105 time and another bioavailable that contains radiocesium in both solute and solid forms (the  
 106 concentrations of which are assumed at instantaneous reversible equilibrium). The predicted  
 107  $TF$  at time  $t$  (in years) is further decomposed as follows:

$$TF(t) = \frac{C_V(t)}{C_S(t)} = \frac{CF}{Kd} \cdot D(t) \quad (2)$$

108 This approach requires the determination of two empirical parameters independent of time:  
 109 the solid liquid distribution coefficient  $Kd$  (in L/kg<sub>dm</sub>) and the concentration factor  $CF$  (in  
 110 L/kg<sub>dm</sub>) defined as the ratio of activity concentration in grass vegetation to that in soil  
 111 solution. The calculation of  $Kd$  and  $CF$  requires knowledge of some soil physico-chemical  
 112 properties. An additional dynamic factor, namely  $D(t)$  (dimensionless), representing the

113 ageing of  $^{137}\text{Cs}$  in the rooting layer, is defined as the percentage of bioavailable  $^{137}\text{Cs}$  with  
114 respect to time. Bioavailability is decreasing over time ( $D$  ranging from 0 to 1) mainly due to  
115 the fixation onto soil particles ( Smith et al., 1999). Here, the decreasing of  $D$  is quite  
116 independent of loss factors such as radioactivity decay, water removal (leaching, run-off),  
117 erosion and removal of harvested biomass since all these factors are already implicitly taken  
118 into account through time dependent of  $^{137}\text{Cs}$ .

### 119 2.1.1. Parameterization of $D(t)$

120 According to IAEA report (IAEA-TECDOC-472, 2010), the bioavailable fraction  $D(t)$  can be  
121 neglected (i.e. sets equal to 1) when comparing  $TF$  for a set of similar soils on mid-term after  
122 a contamination event. However, this assumption might be invalid when predicting the long  
123 term behavior of radiocesium. In their model, Absalom et al. (1999) assumed that the  
124 decrease of bioavailability depends on the time elapsed between the date of observation ( $t$ )  
125 and the date of the initial deposition ( $t_0$ ), and therefore on the age of contamination in soil ( $t -$   
126  $t_0$ ). More precisely, the bioavailable fraction  $D$  depends only on  $(t - t_0)$ .  $D$  is, therefore,  
127 supposed to be "invariant with time" since it does not depend on  $t_0$  but rather on  $(t - t_0)$ . They  
128 also assumed that the decrease of bioavailable radiocesium in soil was characterized by two  
129 consecutive fast and slow rates described by a first order kinetic equation. In the case of a  
130 single contamination episode taking place on date  $t_0$ ,  $D(t - t_0)$  is given by equation (3):

$$D(t - t_0) = P_{fast} \cdot \exp(-k_{fast} \cdot (t - t_0)) \\ + (1 - P_{fast}) \cdot \exp(-k_{slow} \cdot (t - t_0)) \quad (3)$$

131 Where,  $k_{fast}$  and  $k_{slow}$  (in  $\text{yr}^{-1}$ ) are the apparent first order kinetic rates for the fast ( $P_{fast}$ ) and  
132 the slow ( $1 - P_{fast}$ ) declining fractions, respectively.  $P_{fast}$  represents the fraction of the (initially  
133 bioavailable) deposited radiocesium which is subject to decay according to the fast  
134 component. However, in the case of French pastures which were contaminated by both the

135 Chernobyl accident in 1986 and the global fallouts of nuclear weapons testing in the 1960s,  
 136 this formulation has to be extrapolated. When  $^{137}\text{Cs}$  is introduced into soil by two consecutive  
 137 contamination events occurring at times  $t_1$  and  $t_2$  respectively, the equation (3) can be  
 138 rewritten as follows:

$$D(t) = \vartheta \cdot D(t - t_1) + (1 - \vartheta) \cdot D(t - t_2) \quad (4)$$

139 Where,  $\vartheta$  (ranging from 0 to 1) quantifies the contribution of Chernobyl fallout to the total  
 140 deposit at the considered site and  $D(t-t_1)$  and  $D(t-t_2)$  are calculated according to equation (3).  
 141 As a result of the time invariance hypothesis (i.e. soil structure and properties do not vary  
 142 significantly over time), it is reasonable to consider that the values of  $P_{fast}$ ,  $k_{fast}$  and  $k_{slow}$   
 143 constants do not change between the two contamination events.

144 To date, there is very little data in literature on  $P_{fast}$ ,  $k_{fast}$  and  $k_{slow}$  values and their associated  
 145 uncertainties due to lack of observed data. In this work, we chose to evaluate these kinetic  
 146 constants using mid and long-term field and literature chronic series of radiocesium in milk  
 147 observed after Chernobyl accident. Indeed, such data are scarce in literature and unavailable  
 148 for grass. Here our calculations were based on the hypothesis reported in literature that the  
 149 radiocesium activity concentration in milk at mid and long terms can change at the same rate  
 150 as the activity concentration in grass which in turn is in equilibrium with the radiocesium  
 151 concentration in soil solution ( Smith et al., 1999; Absalom et al., 1999; Brimo et al., 2019).

152 Mathematically, the rates of change in the radiocesium content of *vegetation pasture or cow*  
 153 *s' milk (M)* can be expressed as follows:

$$\frac{C_M(t)}{C_{M,t0}} = P_{fast} \cdot \exp(-(\lambda_{fast}^M + \lambda) \cdot t) + (1 - P_{fast}) \cdot \exp(-(\lambda_{slow}^M + \lambda) \cdot t) \quad (5)$$

154 Where  $C_M$  is the total activity concentration in  $M$  at time  $t$ ,  $C_{M,t_0}$  denotes the initial radiocesium  
155 concentration in  $M$  after the very short-term transfer processes such as atmospheric deposition and  
156 weathering of radiocesium intercepted by vegetation are were ceased.  $\lambda$  is the physical decay rate  
157 ( $2.31 \times 10^{-2} \text{ yr}^{-1}$ ),  $P_{fast}$  is the same as that involved in Eq. 3 and  $\lambda_{fast}^M$  and  $\lambda_{slow}^M$  are the fast and  
158 slow decline rates (physical decay excluded) for the fast and slow declining fractions  
159 respectively, mainly caused by the combined effects of the radiocesium fixation on specific  
160 and non-specific sites, the leaching of the upper rooting layer by downward infiltration, the  
161 soil erosion and the grazing consecutive to grass uptake (Brimo et al., 2019). On the other  
162 hand, the rates of change in the total radiocesium content of soil (i.e. the sum of bioavailable  
163 and non-bioavailable fractions) are usually described by assuming that the decline in  
164 radioactivity concentration,  $C_S$ , is exponential (i.e.  $C_S \propto \exp(-(\lambda^{soil} + \lambda) \cdot t)$ ).  $\lambda^{soil}$  is  
165 subject to the same aforementioned loss processes as  $\lambda_{fast}^M$  and  $\lambda_{slow}^M$  excluding the fixation  
166 contribution. Here, if the contribution of the environmental processes other than physical  
167 decay is small compared to the contribution of fixation,  $C_S$  would then change with a single  
168 rate close to the physical decay (i.e.  $\lambda^{soil} = \lambda_{fast}^{soil} = \lambda_{slow}^{soil}$ ). Thus, based on above analysis,  
169 we first determined the values of the 3 constants ( $P_{fast}, \lambda_{fast}^M, \lambda_{slow}^M$ ) by analyzing the decrease  
170 of radiocesium activity in milk (i.e.  $M=milk$ ) observed in several European countries (see  
171 section 2.2.2). The constants of the bioavailable fraction  $k_{fast}$  and  $k_{slow}$  required in Eq. 3 were  
172 then deduced as follows:

$$k_{fast} = \lambda_{fast}^{milk} - \lambda^{soil} \quad (6)$$

$$k_{slow} = \lambda_{slow}^{milk} - \lambda^{soil} \quad (7)$$

173

174

### 175 2.1.2. Parameterization of $CF$ and $Kd$

176 Calculation of  $CF$  and  $Kd$  relies on the knowledge of soil properties including clay content,  
177 pH, organic matter content (OM), cation exchange capacity (CEC) and exchangeable  
178 potassium (K) concentration. In the present work, the calculation of  $CF$  was performed by  
179 testing different semi-mechanistic formulations derived by Smolders et al. (1997), Absalom  
180 et al. (1999), Absalom et al. (2001) or Tarsitano et al. (2011). Similarly, the parameter  $Kd$  was  
181 estimated based on one of the following models: Absalom et al. (1999), Absalom et al. (2001)  
182 , Tarsitano et al. (2011) or Uematsu et al. (2015). The sets of mathematical equations with  
183 their default parameter values are summarized in Supplementary Information (SI). These  
184 equations differ by their mathematical formulation, the required input soil properties and also  
185 by the type of soils for which they were developed. While the equation of Uematsu et al.  
186 (2015) was mainly derived using agricultural Japanese soils from the Fukushima affected  
187 areas, all other equations were derived on the basis of data mostly acquired in laboratory  
188 experiments. These latter were carried out on mineral soils collected from European  
189 grasslands and have lasted over periods of several weeks to several months (i.e. the cases of  
190 Absalom et al. (1999) and Smolders et al. (1997)). However, in addition to the mineral soils,  
191 the equations given by Absalom et al. (2001) and Tarsitano et al. (2011) were parameterized  
192 using additional field data obtained for soils with high organic matter contents.

## 193 2.2. Field data

### 194 2.2.1. Data used for calibrating $D(t)$

195 As listed in Table 1, it consists of 10 different long term monitoring series of  $^{137}\text{Cs}$  activity  
196 concentrations in cow's milk, mostly acquired in grazing areas in France. The data acquired in  
197 France were for a part already described in Brimo et al. (2019) and for the other part  
198 unpublished (i.e. Puy de Dôme). To enrich the dataset, we further included time series of the  
199 aggregated transfer coefficients ( $T_{ag}$ ) of  $^{137}\text{Cs}$  activity in milk acquired from 1986 to 1999 in

200 three other European countries (Austria, Czech Republic and Germany) and compiled in  
 201 Mück (2003). Overall, we had access to about 200 measurements that covered the entire  
 202 period from 1986 to 2017.

203

204

205 **Table 1:** Description of the milk time series used to estimate the values of  $P_{fast}$ ,  $k_{fast}$  and  $k_{slow}$

| Source                            | Location        | Observation period | Nb. of observations ( $n$ ) |
|-----------------------------------|-----------------|--------------------|-----------------------------|
| Mück (2003)                       | Austria         | 1986-1999          | 12                          |
|                                   | Germany         | 1986-1999          | 12                          |
|                                   | Czech Republic  | 1986-1999          | 14                          |
| This study<br>Brimo et al. (2019) | France          |                    |                             |
|                                   | Puy de Dôme     | 1986-1999          | 52                          |
|                                   | Beaune-le-Froid | 1993-2016          | 22                          |
|                                   | Crey-Malville   | 1996-2016          | 14                          |
|                                   | Cruas           | 1994-2016          | 18                          |
|                                   | Tricastin       | 2000-2015          | 10                          |
|                                   | Chooz           | 1992-2016          | 24                          |
|                                   | Mercantour      | 1999-2017          | 18                          |

206

### 207 2.2.2. Data used for testing $TF$ models

208 The data set selected for testing  $TF$  model performances is independent from that used for  
 209 estimating the bioavailability decay constants in the previous section. The model  
 210 performances were evaluated against data acquired in different grazing areas in France.  
 211 Overall, 101 pasture soils were sampled from 2004 to 2017. Most soils originated from two  
 212 areas: Jura (56 samples from 9 monitoring stations) and Puy de Dôme (19 samples from 3  
 213 monitoring stations) located respectively in eastern and central part of France. The 26 other

214 soil samples were taken in the vicinity of some nuclear power plants (the soil samples not  
215 originated from Puy de Dôme or Jura are denoted NPP hereafter), in the course of radiological  
216 monitoring programs carried out by IRSN. The contribution of the NPP releases to the  
217 contamination of soils in these areas was considered negligible (Duffa et al., 2004), the main  
218 sources remaining, as underlined before, the Chernobyl accident and the nuclear tests. In  
219 addition to the soil physicochemical properties,  $^{137}\text{Cs}$  activity concentration was determined in  
220 the upper soil (0-5 cm) and grass (stems and shoots) from which we calculated the transfer  
221 factors. Methodologies adopted for sampling, preparation of samples and  $^{137}\text{Cs}$  analyses are  
222 detailed in a previous work (Brimo et al., 2019).

223 Table S3 in SI shows in details sampling date, location, observed  $TF$  and the physiochemical  
224 properties (pH, clay content, organic matter content, cation exchangeable capacity,  
225 exchangeable K) of the 101 soil samples. The values of the observed  $^{137}\text{Cs}$  in soil ranged from  
226 2.3 to 103 Bq/kg, the observed  $^{137}\text{Cs}$  in grass from 0.045 to 13.9 Bq/kg, the clay content from  
227 0.05 to 0.56 g/g, the organic matter content from 0.02 to 0.44 g/g, the pH in soil solution from  
228 4.4 to 7.7, the exchangeable K from 0.04 to 2.53 cmol/kg and the CEC from 0.42 to 50.3  
229 cmol/kg. In Puy de Dome, the soil was loamy with high organic matter content (i.e.  $\text{OM} \geq$   
230 20%) whereas it was loamy with low OM content in NPP sites. In the Jura region, the soil  
231 varied between organic (16%), loamy (29%) and clay soils (55%) (IAEA classification  
232 (IAEA-TECDOC-472, 2010)).

### 233 **2.3. Modelling methodology**

#### 234 *2.3.1. Determination of the bioavailability factor constants*

235 Based on the hypothesis of the independence of the bioavailability decay constants ( $P_{fast}$ ,  $k_{fast}$ ,  
236  $k_{slow}$ ) upon the considered site, two different approaches were used to determine them. In the  
237 first approach, the determination was accomplished by considering only the relatively short  
238 time series extending from 1986 to 1999 (i.e. Austria, Germany, Czech Republic and Puy de

239 Dôme). In the second approach, we took into account all the series in order to evaluate the  
240 influence of long term data on the estimates. In order to avoid any bias in the results, we  
241 ignored  $^{137}\text{Cs}$  measurements recorded in 1986 since they were considered highly impacted by  
242 the foliar uptake pathway. On the other hand, we took into account the variability of the initial  
243 activity levels between sites since they were not contaminated at the same deposit level. We  
244 chose to treat the initial activity levels (i.e.  $C_{M,t0}$ ) for every selected time series as extra  
245 constants and they were, therefore, adjusted simultaneously with the bioavailability constants.  
246 Consequently, 7 constants (i.e.  $P_{fast}$ ,  $k_{fast}$ ,  $k_{slow}$  + 4 initial activity levels of the used chronic  
247 time series) needed to be determined in the first approach versus 13 (3+10) in the second  
248 approach. To fit the values of these constants, we implemented equations 5, 6 and 7 in  
249 Matlab. The value of  $\lambda^{soil}$  that is required for deduction  $k_{fast}$  and  $k_{slow}$  values was set to  
250  $0.017 \pm 0.005 \text{ yr}^{-1}$  taken from our former work (Brimo et al., 2019). We used the algorithm  
251 DREAM based on the Bayesian approach to fit the whole constants with their associated  
252 uncertainty. DREAM uses adapted Markov chain Monte-Carlo method that exhibits excellent  
253 sampling efficiencies on high dimensional posterior distributions (Vrugt, 2016). An  
254 aggregated logarithmic mean square error as described by Brown and Dvarzhak (2019) was  
255 chosen as a likelihood function. The algorithm was run with uniform prior distributions  
256 (Table 2). The initial time ( $t_0$ ) was set to May 01, 1986, and was assumed to be the beginning  
257 of  $^{137}\text{Cs}$  deposit for all sites. Except for Puy de Dôme, the constants  $P_{fast}$ ,  $k_{fast}$  were set to zeros  
258 (i.e. prior=posterior=0) for all French time series because these did not exhibit any rapidly  
259 decaying fraction as they started in the early 1990's (i.e. more than 6 years after Chernobyl).

### 260 2.3.2. Calculation of TFs with semi-mechanistic models

261 Based on the estimated values of the bioavailability decay constants (mean  $\pm$  SD) and the  
262 correlations in-between them, the soil-to-plant transfer factor was calculated for each of the  
263 101 samples through Monte-Carlo simulations ( $2.5 \times 10^5$  runs), taking into account

264 uncertainties in  $D$ ,  $CF$  and  $Kd$ . The simulations were run by setting the Chernobyl deposit ( $t_1$ )  
265 to May 01, 1986, whereas the global fallout ( $t_2$ ) was assumed uncertain with a deposition date  
266 being uniformly randomly distributed between January 01, 1960, and December 31, 1965,  
267 since most of atmospheric deposits had occurred by that period (Renaud and Louvat, 2004) .  
268 The values of  $\vartheta$  (mean  $\pm$  SD) were derived from maps provided by Roussel-Debet et al.  
269 (2007) (Table S3 in SI). Each  $\vartheta$  value represents the arithmetical mean of  $\vartheta$  values taken  
270 within area delineated by a circle having a diameter of 30 km around the sampling  
271 coordinates. Indeed, these maps are reliable at regional scales but much less reliable at  
272 smaller spatial scales, for kilometric to deca-kilometric scales. This is why we chose such a  
273 diameter to be big enough but with avoiding overlapping between two adjacent circles.  
274 Simulations with  $\vartheta$  values derived from 60 km circles were also carried out for comparison  
275 purpose but the final results did not show any difference.  $CF$  and  $Kd$  values were estimated  
276 using different alternative models or combinations of models. : In addition to the 3 classical  
277 models (i.e. M1, M2, M3) of Absalom et al. (1999), Absalom et al. (2001) and Tarsitano et al.  
278 (2011), 3 other alternatives (i.e. M4, M5, M6) were tested by using the equation of Smolders  
279 et al. (1997) to estimate  $CF$  while keeping the calculation of  $Kd$  according to the 3 previous  
280 classical original models. Three other alternatives (i.e. M7, M8, M9) were performed by  
281 calculating  $Kd$  on the basis of the  $RIP^{soil}$  (i.e. Radiocesium Interception Potential in soil)  
282 equation reported by Uematsu et al. (2015) while keeping the calculation of  $CF$  according to  
283 the 3 previous classical models. Consequently, 9 different models were tested.

### 284 2.3.3. Assessment of the model performances

285 In order to quantitatively assess model performances, the difference between the predicted  
286 and observed  $TFs$  were quantified by the following statistical indexes: the correlation  
287 coefficient ( $r$ ) using log transformed data, the *Contained* index (%) by calculating the  
288 percentage of observed data inside the predicted bounds and the predicted-to-observed value

289 ratio denoted  $\overline{\text{sim}}/\text{obs}$ . The latter was calculated as follows: the ratio of the predicted median  
290 value to the observed one was first calculated for each sample, from which a median ratio was  
291 calculated. The best performance is assessed by: a close to  $\pm 1$   $r$  values, close to 100 %  
292 *Contained* values and close to 1 ratio  $\overline{\text{sim}}/\text{obs}$  values.

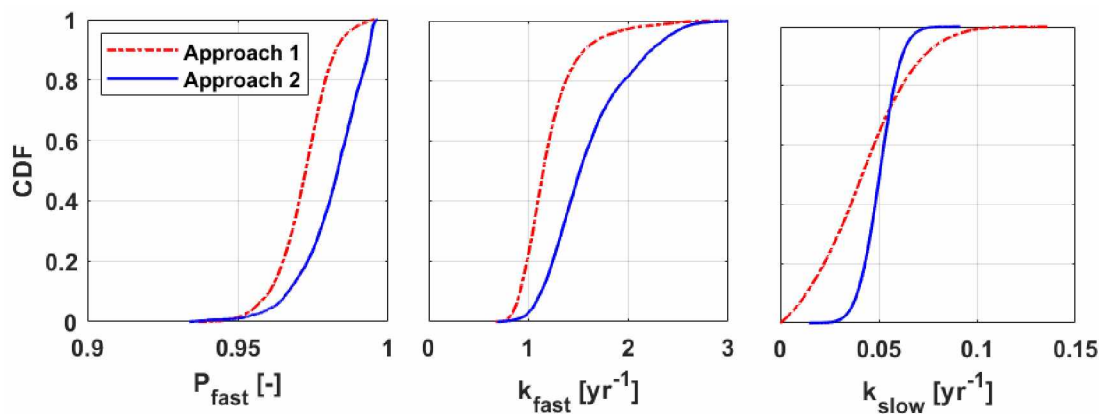
### 293 **3. Results and discussion**

#### 294 **3.1. Bioavailable fraction constants**

295 XXX Table 2 compares the estimates of the posterior mean (Mean) and standard deviation  
296 (SD) of  $P_{fast}$ ,  $k_{fast}$  and  $k_{slow}$  constants for the two approaches. The corresponding posterior  
297 cumulative distribution functions (CDFs) are displayed in Fig 1. The posterior CDFs are well  
298 defined and occupy small ranges within the uniform prior distributions, suggesting that the  
299 data used included sufficient information to calibrate  $D$ . This is also confirmed by the nearly  
300 Gaussian distributions of  $k_{fast}$  and  $k_{slow}$ . The distribution of  $P_{fast}$  appears to depart from  
301 Gaussian and concentrates at its upper possible bound (Fig 2). Results show that  $k_{fast}$  and  $k_{slow}$   
302 given by approach 2 were 1.2-1.3 times higher than that given by approach 1 (Table 1).  
303 However, taking the uncertainties associated with constants into account, this difference  
304 seems slight and is due to difference in the selected time series used as calibration data. The  
305 effective mid-term half-lives  $\left(\frac{\ln 2}{k_{fast}+\lambda}\right)$  amount to  $0.59\pm 0.12$  yr for approach 1 and  $0.46\pm 0.11$   
306 yr for approach 2, while the effective long-term half-lives  $\left(\frac{\ln 2}{k_{slow}+\lambda}\right)$  amount to  $12.05\pm 4.88$  yr  
307 and  $9.57\pm 1.12$  yr, respectively. The ratio  $k_{fast}/k_{slow}$  is approximately the same for the two  
308 approaches, i.e. 31 and 32. The relatively short half-lives estimated for the fast component  
309 suggests that fixation of the bioavailable  $^{137}\text{Cs}$  starts during the first few weeks to months  
310 after initial deposition. This finding is consistent with the opinion of Frissel et al. (2002) who  
311 concluded that 1 year could be enough for  $^{137}\text{Cs}$  fixation in soil. Both approaches give a very

312 high value around 0.97 for the fast-declining fraction ( $P_{fast}$ ) which means that  $^{137}\text{Cs}$   
 313 bioavailability for the investigated soils has decreased drastically within 2 years after the  
 314 accident. Our constant estimations differ from the very few values reported in literature.  
 315 Tarsitano et al. (2011) dropped out the rapid term (i.e.  $P_{fast}=k_{fast}=0$ ) from their version of  
 316 equation (3) arguing that this term was not necessary. However, their hypothesis seems not  
 317 realistic in our case since the two decline phases are obvious for European soils contaminated  
 318 by Chernobyl fallouts (Fig. 2). Our findings of  $k_{fast}$  and  $k_{slow}$  are respectively 1.8-2.3 times  
 319 higher and 0.6-0.7 times lower than the corresponding values reported by Absalom et al.  
 320 (1999) (i.e.  $k_{fast}$  and  $k_{slow}$  of 0.69 and 0.069  $\text{yr}^{-1}$  respectively). Furthermore, these authors  
 321 estimated a value of 0.81 for  $P_{fast}$  which is far away from the lower end of the range of values  
 322 obtained by the present study (see Fig 1). A possible reason of this lower  $P_{fast}$  value is that  
 323 Absalom et al. (1999) chose to optimize this single parameter using imposed values for  $k_{fast}$   
 324 and  $k_{slow}$  despite the correlation among the three parameters (e.g.  $r= 0.8$  between  $P_{fast}$  and  
 325  $k_{fast}$ ). Another possible reason is that  $P_{fast}$  value reported by Absalom and co-authors might  
 326 have been estimated based on data impacted by foliar uptake. Indeed, two of the data sets  
 327 used in  $P_{fast}$  optimization involved data observed in 1986, soon after Chernobyl accident (see  
 328 Table 1 in Absalom et al. (1999)).

329



330

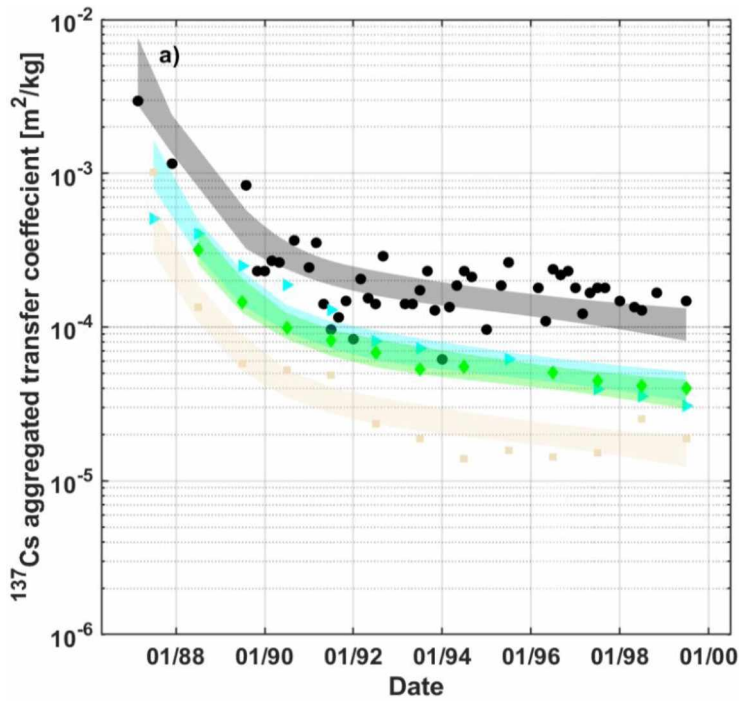
331 **Fig 1:** Posterior CDFs of  $P_{fast}$ ,  $k_{fast}$  and  $k_{slow}$  parameter values given by the two calibration approaches.

332 **Table 2:** Mean and standard deviation (SD) values of the bioavailability decay constants derived by  
 333 the two calibration approaches.

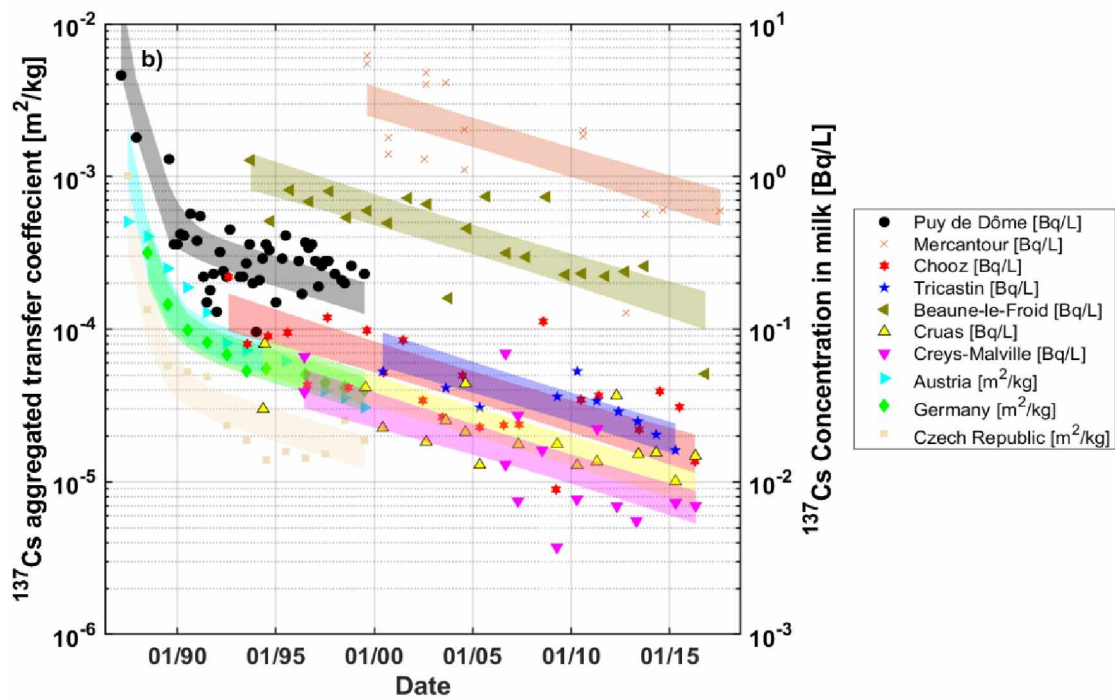
| Parameter  | Unit      | Searching range | Approach 1 |       | Approach 2 |       |
|------------|-----------|-----------------|------------|-------|------------|-------|
|            |           |                 | Mean       | SD    | Mean       | SD    |
| $P_{fast}$ | -         | [0-1]           | 0.97       | 0.009 | 0.98       | 0.011 |
| $k_{fast}$ | $yr^{-1}$ | [0-6]           | 1.21       | 0.263 | 1.60       | 0.416 |
| $k_{slow}$ | $yr^{-1}$ | [0-1]           | 0.043      | 0.022 | 0.050      | 0.009 |

334  
 335 The comparison between the observed and the predicted activity concentrations in cow's milk  
 336 based on calibrated constants are displayed in Fig 2 for the two calibration approaches  
 337 mentioned above. Satisfactory fits to the observed data were found for both approaches, with  
 338  $r$  values varying between 0.69 (n=24) and 1 (n=12) with values being greater than 0.8 for all  
 339 1986-1999 time series. The observations of these latter confirm the hypothesis of a two-phase  
 340 decrease with time. Despite different environmental conditions, the decay rates observed in  
 341 France (Puy de Dôme), Germany, Czech Republic and to some extent in Austria are very  
 342 similar as illustrated by the near-parallel lines of decreasing radioactivity concentrations in  
 343 cow's milk (Fig 2). This was statistically validated with  
 344 ANOVA, Turkey's multiple comparison analysis tests. For this purpose, the previous  
 345 constants were calibrated for each single country individually (results not shown). The  $p$   
 346 values yielded by the statistical test indicated no significant difference between the four  
 347 European countries ( $p$ -values of 0.42, 0.15 and 0.59 for  $P_{fast}$ ,  $k_{fast}$  and  $k_{slow}$  respectively).  
 348 Therefore, our results indicate that literature data do not call into question the present  
 349 assumption that bioavailability decay constants can be considered as site-independent.

350  
 351  
 352



353



354

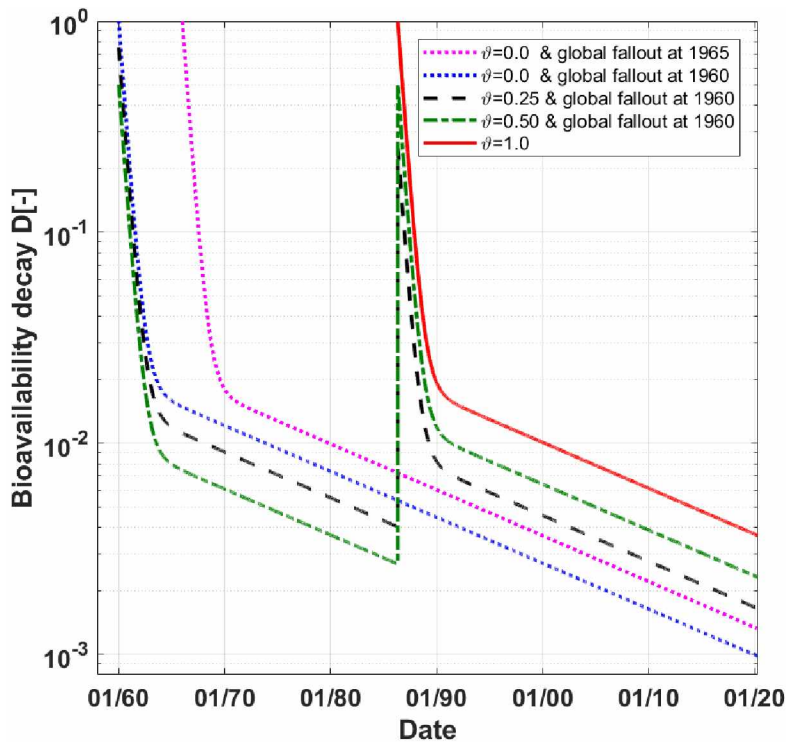
355 Fig 2: Comparison between observed (symbols) and predicted (line) values of the  $^{137}\text{Cs}$  activity  
 356 concentration in cow milk (normalized by the deposit for Austria, Germany and Czech Republic): (a)  
 357 with long-term time series excluded (approach 1), (b) with all series being considered (approach 2).

358 Based on the above discussion and taking into account that the semi-mechanistic models will  
 359 be tested against field data acquired 20 to 30 years after Chernobyl accident, we chose to

360 calculate the bioavailability decay  $D$  using the decay constants given by approach 2. The time  
361 evolution of the predicted bioavailability decay is illustrated graphically in Fig.3 for varying  
362 contributions of Chernobyl fallouts to the total deposit (i.e.  $\vartheta = 0.0, 0.25, 0.5, 1.0$ ). Regardless  
363 of  $\vartheta$  value, results show that the predicted percentage of bioavailable  $^{137}\text{Cs}$  in soil at present  
364 year (i.e. 2020) is actually very low ( $D = 0.1 \%, 0.17 \%, 0.23 \%, 0.4 \%$  for  $\vartheta = 0.0, 0.25, 0.5,$   
365  $1.0$  respectively). The contribution of Chernobyl to the bioavailable radiocesium present in  
366 soil is thus 4 times higher than that of the global fallouts (by excluding the effects of other  
367 environmental processes and radioactivity decay). On the other hand, the date of the global  
368 fallout deposit appears to have a negligible impact on the predicted value. Results further  
369 show that the predicted  $D$ 's attributed to the global fallout (i.e.  $\vartheta = 0.0$ ) is almost the same  
370 whether deposit occurs in 1960 or 1965 (0.10 % versus 0.13 % respectively). This finding  
371 suggests, thus, setting the deposition of  $^{137}\text{Cs}$  from global fallout to a punctual deposit in the  
372 modeling studies of long term  $^{137}\text{Cs}$  fate.

373

374



375

376 **Fig 3:** Illustration of changes in radiocesium bioavailable fraction ( $D$ ) in a pasture soil for different  
 377 levels of contribution of Chernobyl fallouts to the total deposit (i.e.  $\vartheta = 0.0, 0.25, 0.5, 1.0$ ). Except the  
 378 magenta pointed line, the simulations were performed by assuming a punctual contamination by global  
 379 fallout occurring at the early 1960. The magenta pointed line illustrates the case of a complete  
 380 punctual contamination by global fallout (i.e.  $\vartheta = 0$ ) occurring in 1965. Constant values ( $P_{fast}$ ,  $k_{fast}$ ,  
 381  $k_{slow}$ ) are those obtained by approach 2 (Table 2).

### 382 3.2. Exploratory analysis of $TFs$ data

383 To determine whether  $TFs$  significantly vary among the different areas we performed  
 384 ANOVA, Turkey's multiple comparison analysis of the log transformed data (Fig S1). The  
 385 statistical test showed no significant difference between Jura and NPP ( $p$ -value= 0.94 > 0.05).  
 386 In contrast, a significant difference was found between Puy de Dôme and the other two areas  
 387 ( $p$ -value= 0.006 and 0.009 respectively). Such results would be partly explained on the basis  
 388 of the soil organic matter (OM) content. This latter was significantly higher in Puy de Dôme  
 389 compared to Jura and NPP (i.e. 63% of samples are with OM content equal or greater than  
 390 20% versus only 16% and 4% for Puy de Dôme, Jura and NPP respectively). The mean

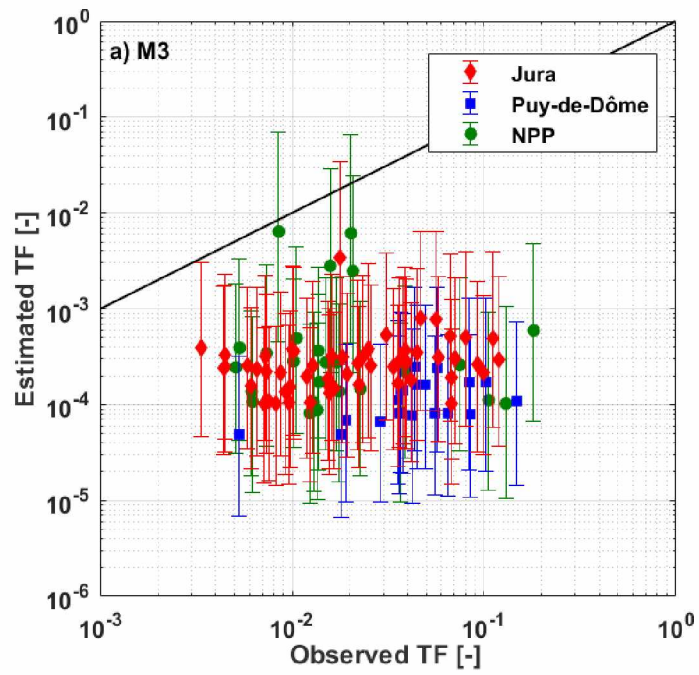
391 observed  $TFs$  have decreased in the same order: Puy de Dôme ( $TF=0.052$ ) > Jura ( $TF=0.036$ )  
392 > NPP ( $TF=0.032$ ). These observations are consistent with previous studies reporting an  
393 increase of  $^{137}Cs$  transfer to plant with increasing OM contents (Noordijk et al., 1992; Rosén  
394 et al., 1999).

395 As indicated in Table S3, the observed  $TFs$  -ranged from 0.003 to 0.18 with a mean value of  
396 0.035. This range is close to the lower bound of the range reported by IAEA for pasture  
397 stems and shoots and the “all soils” group, i.e.  $TFs$  values within the range 0.01 - 5 and a  
398 mean value of 0.25 (IAEA-TECDOC-472, 2010). Such low observed  $TFs$  might be explained  
399 by the reduction of  $^{137}Cs$  bioavailability with increasing elapsed time since the initial  
400 deposition. Indeed, while data compiled by IAEA were mostly relied on studies carried a few  
401 years after Chernobyl accident, the present data were collected from 20 to 30 years after  
402 Chernobyl and more than 50 years after global fallouts. As indicated in Fig. 3, one would note  
403 that even for a site exclusively contaminated b by Chernobyl (i.e.  $\vartheta=1$ ), the bioavailability  
404 fraction predicted 20 to 30 years after deposition is 0.7 % and 0.4 % respectively which are  
405 actually very much lower than 100. Hence the current low  $TFs$  with respect to the range  
406 compiled by IAEA is accounted by the diminishing of the soil bioavailability, more than 30  
407 years after the contamination.

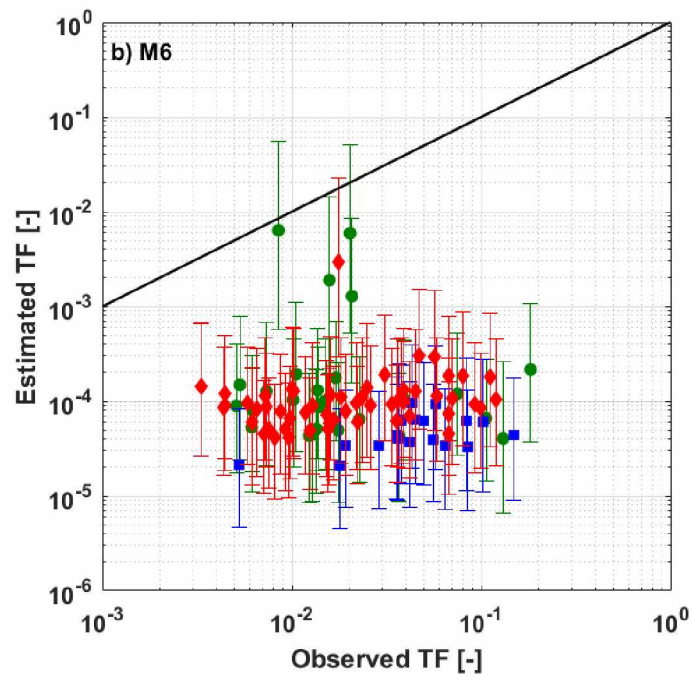
### 408 **3.3. Predicted versus observed $TFs$**

409 Scatter diagrams showing modeled against observed  $TFs$  for models (M3, M6 and M9 are  
410 shown in Fig 4. Results for the remaining models are presented in Fig S2 in SI. Table 3  
411 summarizes the averages and the confidence intervals of  $CF$  and  $Kd$  estimates for the various  
412 models (see section 2.3.2). Since  $D$  estimates do not differ between models, they are not  
413 presented here. Among the 101 observations, its value ranged from 0.001 to 0.005, with a  
414 median at 0.004.

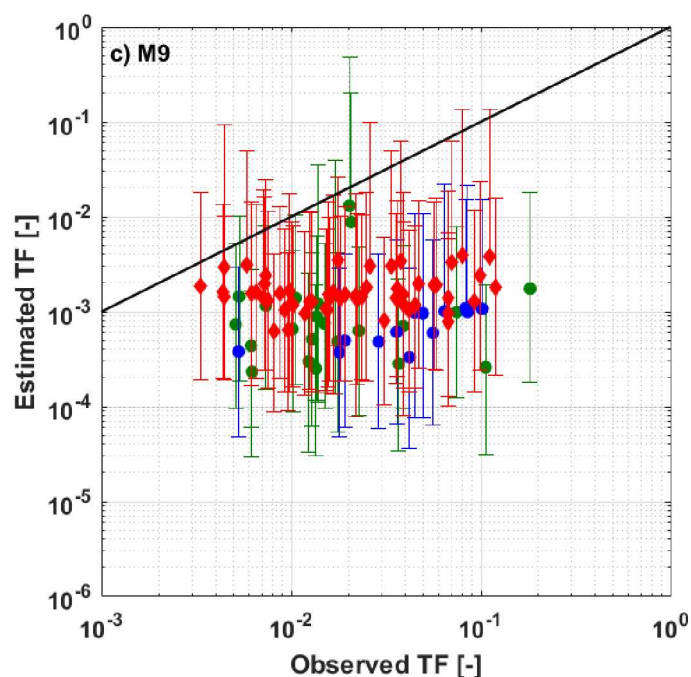
415



416



417



418

419 **Fig 4:** Predicted (95 CI.) versus observed value of the soil-to-grass transfer factor  $TF$  for the 101  
 420 samples using: a) model 3, b) model 6, c) model 9. Solid line represents the 1:1 relationship.

421 Thereafter we use the results of the nine models to evaluate their performances by  
 422 differentiating three families of models: the “original” ones (Absalom et al. (1999), Absalom  
 423 et al. (2001) and Tarsitano et al. (2011)), the ones based on a  $CF$  estimated by Smolders et al.,  
 424 (1997) and the last 3 ones based on  $RIP^{soil}$  estimated by Uematsu et al. (2015).

425 *Original models M1, M2 and M3*

426 Table 4 summarizes the statistics of the performances of the tested models. In general terms,  
 427 results show that the 3 models are as bad as each other in replicating the observations. M2  
 428 shows a slightly better agreement with observations as confirmed with *Contained* index of  
 429 56%. Nevertheless, a very poor agreement between observed and predicted  $TFs$  could still be  
 430 appeared. Fig 4a clearly illustrates that the  $TFs$  estimates by M3 are almost 2 orders of  
 431 magnitude lower than the observed ones. Additionally, no improvement could be found in  
 432 terms of model ability to describe the variability among sampling soils.

433 *Models based on CF from Smolders et al. (1997): M4, M5 and M6*

434 Results show that application of this parameterization of *CF* leads to a poorer clustering  
435 around the 1:1 line than the previous models because the estimated *CFs* were generally lower  
436 than those estimated by the original models by a factor of 2 in average (Fig 4b and Table 3).  
437 The variability between the sites is also not better explained with these alternative models as  
438 confirmed with the poor correlation coefficients (Table 4).

439 *Models based on a RIPsoil from Uematsu et al. (2015): M7, M8 and M9*

440 Results show that using the radiocesium interception potential ( $RIP^{soil}$ ) for *Kd* calculation has  
441 significantly improved the model fits when compared to the previous ones. This improvement  
442 is ascribed to the large reduction in *Kd* values of about ~ 5-7 times compared to the original  
443 formulations. The relatively high value of 95 % for *Contained* index obtained by M8 is  
444 attributable to the high uncertainty in model outputs due to the high uncertainty associated  
445 with the input parameters of the corresponding models. Among all the models, the best  
446 clustering around the 1:1 line was found in M9 with a  $\overline{sim}/obs$  ratio of 0.06. However, the  
447 matching remains very poor and unconvincing. The relatively high correlation ( $r=0.76$ )  
448 observed for Puy de Dôme sites is likely due to the number of observations which was smaller  
449 than in other cases ( $N=13$  compared to  $N=19$ ). Indeed, application of Uematsu's  
450 parameterization to these sites produced some negative values for 3 and 7 samples from NPP  
451 and Puy de Dôme respectively, suggesting that this equation which was calibrated for  
452 Japanese soils might not be suitable for European soils.

453 To summarize, we would say that, while the observed *TF* display a wide range of variability  
454 (by a factor of 30, typically), the predicted *TF* do not vary significantly among sites, and  
455 remain relatively constant for a given region (Jura, Puy de Dôme, NPP). This demonstrates  
456 that the variability was poorly explained by any of these 9 models, although slightly better in

457 Puy de Dôme region. The second important result is that predicted *TFs* are systematically  
 458 biased, and remain far below the observed ones, by one to two orders of magnitude, typically.  
 459 These results argue therefore against the usefulness of the semi-mechanistic models to  
 460 accurately predict the long-term soil-to-grass transfer of <sup>137</sup>Cs in the French pastures under  
 461 investigation.

462 **Table 3:** Summary of *CF* and *Kd* values calculated with the various models

| Model             | Description   | <i>CF</i> (L/kg <sub>dm</sub> )                        | <i>Kd</i> (L/kg <sub>dm</sub> )                        |
|-------------------|---|--|--|
| M1 <sup>a,b</sup> | <i>CF</i> (Absalom et al., 1999)<br><i>Kd</i> (Absalom et al., 1999)  | $[2.7x 10^1 - 3.0x 10^4]$<br>$\overline{5.5 x 10^2}$   | $[6.1x 10^2 - 3.5 x 10^5]$<br>$\overline{4.8 x 10^4}$  |
| M2 <sup>a,b</sup> | <i>CF</i> (Absalom et al., 2001)<br><i>Kd</i> (Absalom et al., 2001)  | $[1.9x 10^1 - 1.2x 10^4]$<br>$\overline{2.6 x 10^2}$   | $[8.6x 10^2 - 2.3 x 10^4]$<br>$\overline{1.0 x 10^4}$  |
| M3 <sup>a,b</sup> | <i>CF</i> (Tarsitano et al., 2011)<br><i>Kd</i> (Tarsitano et al., 2011)  | $[7.0 x 10^1 - 4.8 x 10^4]$<br>$\overline{7.4 x 10^2}$ | $[9.3 x 10^2 - 4.8 x 10^4]$<br>$\overline{1.5 x 10^4}$ |
| M4 <sup>a,b</sup> | <i>CF</i> (Smolders et al., 1997)<br><i>Kd</i> (Absalom et al., 1999)   | $[6.3 x 10^1 - 5.9x10^3]$<br>$\overline{3.0 x 10^2}$   | $[6.1 x 10^2 - 3.5 x 10^5]$<br>$\overline{4.8 x 10^4}$ |
| M5 <sup>a,b</sup> | <i>CF</i> (Smolders et al., 1997)<br><i>Kd</i> (Absalom et al., 2001)   | $[3.8 x 10^1 - 4.0 x 10^4]$<br>$\overline{2.6 x 10^2}$ | $[8.6 x 10^2 - 2.3 x 10^4]$<br>$\overline{1.0 x 10^4}$ |
| M6 <sup>a,b</sup> | <i>CF</i> (Smolders et al., 1997)<br><i>Kd</i> (Tarsitano et al., 2011)   | $[4.9 x 10^1 - 4.6 x 10^4]$<br>$\overline{2.7x 10^2}$  | $[9.3 x 10^2 - 4.8 x 10^4]$<br>$\overline{1.5 x 10^4}$ |
| M7 <sup>a,c</sup> | <i>CF</i> (Absalom et al., 1999)<br>RIP <sub>soil</sub> (Uematsu et al., 2015)<br><i>Kd</i> = RIP <sub>soil</sub> /mk   | $[2.7 x 10^1 - 3.0 x 10^4]$<br>$\overline{6.4 x 10^2}$ | $[5.2 x 10^2 - 4.4 x 10^4]$<br>$\overline{6.5 x 10^3}$ |
| M8 <sup>a,c</sup> | <i>CF</i> (Absalom et al., 2001)<br>RIP <sub>soil</sub> (Uematsu et al., 2015)<br><i>Kd</i> = RIP <sub>soil</sub> /mk   | $[1.9 x 10^1 - 9.6 x 10^3]$<br>$\overline{2.3 x 10^2}$ | $[2.2 x 10^2 - 3.5 x 10^4]$<br>$\overline{2.1 x 10^3}$ |
| M9 <sup>a,c</sup> | <i>CF</i> (Tarsitano et al., 2011)<br>RIP <sub>soil</sub> (Uematsu et al., 2015)<br><i>Kd</i> = RIP <sub>soil</sub> /mk | $[7.0 x 10^1 - 4.5x 10^4]$<br>$\overline{9.3 x 10^2}$  | $[1.8 x 10^2 - 5.3 x 10^4]$<br>$\overline{2.8 x 10^3}$ |

463 <sup>a</sup> Median values are overlined while 95CI values are given in brackets

464 <sup>b</sup> Number of observations n=101

465 <sup>c</sup> Number of observations n=92

466 **Table 4:** Model performance indexes for predicted *TF*

| Statistic  | Site        | Models          |                 |                 |                 |                 |                 |                 |                 |                 |
|--|-------------|-----------------|-----------------|-----------------|-----------------|-----------------|-----------------|-----------------|-----------------|-----------------|
|  |             | M1 <sup>a</sup> | M2 <sup>a</sup> | M3 <sup>a</sup> | M4 <sup>a</sup> | M5 <sup>a</sup> | M6 <sup>a</sup> | M7 <sup>b</sup> | M8 <sup>b</sup> | M9 <sup>b</sup> |
| <i>r</i>   | NPP         | -0.13           | -0.01           | -0.1            | -0.04           | -0.03           | -0.09           | -0.06           | 0.16            | 0.07            |
|  | Puy de Dôme | 0.52            | 0.53            | 0.54            | 0.34            | 0.52            | 0.50            | 0.67            | 0.70            | 0.76            |
|  | Jura        | 0.29            | 0.29            | 0.24            | 0.31            | 0.27            | 0.21            | 0.15            | 0.10            | 0.15            |
|  | All         | -0.07           | 0.05            | -0.04           | -0.02           | 0.02            | -0.05           | -0.05           | 0.08            | 0.06            |
| Contained (%)  | NPP         | 0.0             | 61.5            | 15.8            | 0.0             | 11.5            | 7.7             | 8.7             | 91.3            | 34.8            |
|  | Puy de Dôme | 0.0             | 10.5            | 0.0             | 0.0             | 0.0             | 0.0             | 0.0             | 84.6            | 0.0             |
|  | Jura        | 0.0             | 69.6            | 1.8             | 0.0             | 0.0             | 1.8             | 0.0             | 100             | 37.5            |
|  | All         | 0.0             | 56.4            | 5.0             | 0.0             | 3.0             | 3.0             | 2.2             | 95.7            | 31.5            |
| ratio $\frac{\overline{\text{sim}}}{\text{obs}}$ (-) | NPP         | 0.007           | 0.0064          | 0.0168          | 0.0039          | 0.0075          | 0.0077          | 0.0124          | 0.0161          | 0.05            |
|  | Puy de Dôme | 0.0004          | 0.0010          | 0.0027          | 0.0004          | 0.0012          | 0.0012          | 0.0029          | 0.0064          | 0.02            |
|  | Jura        | 0.0023          | 0.0047          | 0.0124          | 0.0012          | 0.0050          | 0.0047          | 0.0230          | 0.0237          | 0.08            |
|  | All         | 0.002           | 0.0037          | 0.0093          | 0.0011          | 0.0041          | 0.0038          | 0.0175          | 0.0193          | 0.06            |

467 <sup>a</sup> Number of observations n=101

468 <sup>b</sup> Number of observations n=92

### 469 3.4. Why models did not fit well the observed data?

470 Assuming that the bioavailability decay ( $D$ ) has been accurately estimated thanks to the  
471 calibration procedure, the low performances of the models could be attributed to the  
472 inaccurate estimations of the  $CF/Kd$  ratio as part of equation (2). Several factors may have  
473 deteriorated the estimates. At first, being semi-empirical models, the use of these models is  
474 usually restricted to the specified (grass and/or soil) data to which they were calibrated. An  
475 extrapolation to other data/sites may result in wrong estimates. An adjustment of their default  
476 parameters might, thus, be required each time we change sites or of data. Additionally, these  
477 models have been mostly calibrated by laboratory data of specific plant species especially  
478 ryegrass and wheat which it is not the case here where a large variety of herbage species was  
479 observed from a sampling plot to another (i.e. such as *poaceae*, *fabaceae*, *ramunculaceae* and  
480 *asteraceae*) (Besson, 2009). This variability is mostly due to the variability of soil  
481 characteristics and climatic conditions. Several studies have highlighted significant  
482 differences in plant uptake of radiocesium among the plant species (Broadley and Willey,  
483 1997; Ciuffo et al., 2003; Lasat et al., 1997). It is possible, therefore, that a significant part of  
484 the observed variability originates in  $CF$  due to the variety of grass species encountered at the  
485 monitoring sites. Another weakness of the models, is that the process of adherence of  
486 contaminated soil particles to the aerial part of the vegetation, which has been reported to  
487 increase significantly the radiocesium content in grass (Beresford and Howard, 1991), is  
488 neglected in the models under consideration.

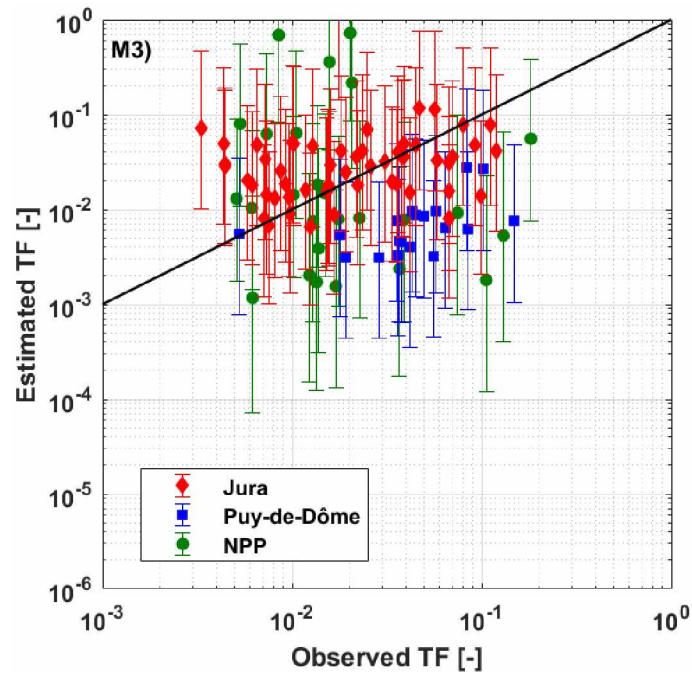
489 Another important reason explaining the discrepancy between observed and predicted  $TF$  is  
490 the extremely high estimated  $Kd$  values, the median values of which range from 2100 to  
491 48000 L/kg<sub>dm</sub> (Table 3). Indeed, the predicted  $Kd$  values are calculated using semi-empirical  
492 equations based on linear correlations which were derived from non-labile  $Kd$  measurements.  
493 These measurements are based on the hypothesis that radiocesium in solution is in

494 instantaneous equilibrium with the solid phase of soil and that the exchanges between these  
495 phases is reversible. However, a fraction of radiocesium may become fixed to the solid phase  
496 due to ageing effects. This may lead to non-labile  $Kd$  values higher by orders of magnitude  
497 than the labile ones. This was shown in Fig 3 where the labile fraction rapidly decreased after  
498 initial deposition due to the rapid decrease of bioavailability in the first few weeks to months  
499 after initial contamination. Results showed that a decrease by more than 98% of the initial  
500 labile fraction would occur after only 44 months following Chernobyl accident, even in the  
501 case of unique source of contamination by Chernobyl.

502 To test this assumption, we carried out additional simulations adopting a constant labile  $Kd$   
503 value of 165 L/kg<sub>dm</sub> as recommended by Roussel-Debet and Colle (2005). The test was  
504 applied on the first six models (i.e. M1, M2, M3, M4, M5, M6). The models M7, M8, and M9  
505 were not included here as they were essentially based on the estimation of  $Kd$  using  $RIP^{soil}$   
506 equation. Results obtained with models M3 are displayed in Fig. 4, while the remaining ones  
507 are displayed in Fig S3 in S.I. Table 5 shows that the best clustering around the 1:1 line was  
508 found with M3 with a ratio  $\overline{sim}/obs$  value of 0.97. Compared to the former models, results  
509 show that the modification of labile  $Kd$  has significantly improved the model performances.  
510 However, no improvement could be found regarding the variability. This is not surprising  
511 since a single value of labile  $Kd$  was imposed for all the sampled soils.

512

513



514

515 **Fig 5:** Predicted (95 CI) versus observed value of the soil-to-plant transfer factor  $TF$  for the 101  
 516 samples, using model M3 with an imposed labile  $Kd$  value of 165 L/kg<sub>dm</sub>. Solid line represents the  
 517 1:1 relationship.

518 **Table 5:** Model performance indexes for predicted  $TF$  with an imposed labile  $Kd$  value of 165  
 519 L/kg<sub>dm</sub>

| Statistic                                    | site        | Models |       |       |       |       |       |
|--|-------------|--------|-------|-------|-------|-------|-------|
|  |             | M1     | M2    | M3    | M4    | M5    | M6    |
| $r$  | NPP         | -0.19  | -0.05 | -0.14 | -0.18 | -0.06 | -0.15 |
|  | Puy de Dôme | 0.35   | 0.53  | 0.47  | 0.34  | 0.54  | 0.47  |
|  | Jura        | 0.14   | 0.21  | 0.16  | 0.12  | 0.20  | 0.14  |
|  | All         | -0.13  | 0.01  | -0.08 | -0.14 | -0.01 | -0.09 |
| Contained (%)                                | NPP         | 42.3   | 100   | 61.5  | 42.3  | 38.6  | 30.8  |
|  | Puy de Dôme | 5.3    | 100   | 57.9  | 5.3   | 5.3   | 5.3   |
|  | Jura        | 71.4   | 100   | 87.5  | 64.3  | 62.5  | 69.6  |
|  | All         | 51.5   | 100   | 75.3  | 47.5  | 45.5  | 47.5  |
| ratio $\overline{\text{sim}}/\text{obs}$ (-) | NPP         | 0.38   | 0.14  | 0.52  | 0.42  | 0.17  | 0.20  |
|  | Puy de Dôme | 0.06   | 0.07  | 0.16  | 0.06  | 0.08  | 0.06  |
|  | Jura        | 1.04   | 0.34  | 1.23  | 0.52  | 0.37  | 0.47  |
|  | All         | 0.66   | 0.24  | 0.97  | 0.36  | 0.28  | 0.37  |

520

521

522 **4. Conclusion**

523 With the aim in mind of improving our understanding of the long-term behavior of  $^{137}\text{Cs}$  in  
524 terrestrial environments, the present paper evaluates existing assessment models against long-  
525 term monitoring data of activity levels observed -between 2004 and 2017- in different French  
526 grazing areas contaminated by global fallouts and Chernobyl accident. The observed soil to  
527 grass transfer factor values (*TFs*) were found to be close to the lower bound of those  
528 synthesized by IAEA and this was explained by the extreme reduction of  $^{137}\text{Cs}$  bioavailability  
529 due to the old contamination of monitoring sites. For this reason, an effort has been carried  
530 out to better quantify the decay of bioavailable radiocesium in soil, using mid-term (10 years  
531 about) and long term (more than 20 years) series of  $^{137}\text{Cs}$  activities in milk observed in 4  
532 European countries after Chernobyl. These enable us to identify a double kinetics of  
533 bioavailability decay with two effective half-lives for the fast and slow declining fractions  
534 which were found to be equal to  $0.46\pm 0.11$  yr and  $9.57\pm 1.12$  yr respectively. Additionally, a  
535 very high value around 0.97 was identified for the fast-declining fraction ( $P_{fast}$ ). A special  
536 attention should have been be paid to bioavailability decay ( $D$ ) not only because inaccurate  
537 estimate of this parameter might lead to significant overestimate of  $^{137}\text{Cs}$  transfer from soil to  
538 grass and thereby in the food chain but also because  $D$  would explain a large part of the  
539 variability observed on *TFs* in literature. However, In spite of this effort, predicted *TFs*  
540 remain by far lower than the observed ones by one to two orders of magnitude typically,  
541 suggesting that  $Kd$  is overestimated by models. Thus, calculation of  $Kd$  should involve easily  
542 exchangeable  $^{137}\text{Cs}$  rather than total soil  $^{137}\text{Cs}$ . This is all the more justified that the non-  
543 exchangeable fraction (i.e. non-labile and non-bioavailable) was already taken into account  
544 through  $D$  (Fig 3), and therefore  $Kd$  has only to concern the easily exchangeable part (labile  
545 and bioavailable). Furthermore, the variability between sites was poorly explained by semi-  
546 mechanical models mostly because, being semi-empirical models, they require a recalibration  
547 of the parameters and coefficients involved in the model each time we change sites or of data.

## 548 **5. Acknowledgements**

549 This work was funded by Institut de Radioprotection et de Sûreté Nucléaire (IRSN) in France,  
550 MEMOREX project. The field work on radiocesium monitoring at some French pasture sites  
551 was undertaken during the PhD program of Benoit Besson. The authors are grateful to Gilles  
552 Salaün for help in data collection. The first author thanks Dr. Marie Simon-Cornu (IRSN) for  
553 reviewing the manuscript prior to submission.

554

## 555 **6. References**

556 Absalom, J.P., Young, S.D., Crout, N.M.J., 1995. Radio- caesium fixation dynamics:  
557 measurement in six Cumbrian soils. *Eur. J. Soil Sci.* 46, 461–469.  
558 <https://doi.org/10.1111/j.1365-2389.1995.tb01342.x>

559 Absalom, J.P., Young, S.D., Crout, N.M.J., Nisbet, A.F., Woodman, R.F.M., Smolders, E.,  
560 Gillett, A.G., 1999. Predicting soil to plant transfer of radiocesium using soil  
561 characteristics. *Environ. Sci. Technol.* 33, 1218–1223.

562 Absalom, J.P., Young, S.D., Crout, N.M.J., Sanchez, A., Wright, S.M., Smolders, E., Nisbet,  
563 A.F., Gillett, A.G., 2001. Predicting the transfer of radiocaesium from organic soils to  
564 plants using soil characteristics. *J. Environ. Radioact.* 52, 31–43.

565 Albers, B.P., Steindl., H., Schimmack., W., Bunzl., K., 2000. Soil-to-plant and plant-to-cow'  
566 s milk transfer of radiocaesium in alpine pastures : significance of seasonal variability.  
567 *Chemosphere* 41, 717–723.

568 Almahayni, T., Beresford, N.A., Crout, N.M.J., Sweeck, L., 2019. Fit-for-purpose modelling  
569 of radiocaesium soil-to-plant transfer for nuclear emergencies: a review. *J. Environ.*  
570 *Radioact.* 201, 58–66. <https://doi.org/10.1016/j.jenvrad.2019.01.006>

571 Beresford., N.A., Howard., B.J., 1991. The importance of soil adhered to vegetation as a  
572 source of radionuclides ingested by grazing animals. *Sci. Total Environ.* 107, 237–254.  
573 [https://doi.org/10.1016/0048-9697\(91\)90261-C](https://doi.org/10.1016/0048-9697(91)90261-C)

574 Besson, B., 2009. Sensibilité radioécologiques des zones de prairie permanentes. PhD thesis.  
575 Université de Franche-Comté Besançon, France.

576 Brimo, K., Gonze, M.A., Pourcelot, L., 2019. Long term decrease of <sup>137</sup>Cs bioavailability in  
577 French pastures : Results from 25 years of monitoring Long term decrease of <sup>137</sup> Cs  
578 bioavailability in French pastures : Results from 25 years of monitoring. *J. Environ.*  
579 *Radioact.* 208–209. <https://doi.org/10.1016/j.jenvrad.2019.106029>

580 Broadley, M.R., Willey, N.J., 1997. Differences in root uptake of radiocaesium by 30 plant  
581 taxa. *Environ. Pollut.* 97, 11–15.

582 Brown, J., Dvarzhak, A., 2019. EJP-CONCERT: D9.61- Guidance to select level of  
583 complexity.

584 Ciuffo, L., Velasco, H., Belli, M., Sansone, U., Transfer, S., 2003. Cs soil-to-plant transfer for  
585 individual species in a semi-natural grassland . Influence of potassium soil content. *J.*  
586 *Radiat. Res.* 283, 277–283.

587 Duffa, C., Masson, M., Gontier, G., Claval, D., Renaud, P., 2004. Synthèse des études  
588 radioécologiques annuelles menées dans l environnement des centrales électronucléaires  
589 françaises depuis 1991. *Radioprotection* 39, 233–254.

590 Frissel, M., Deb, D., Fathony, M., Lin, Y., Mollah, A., Ngo, N., Othman, I., Robison, W.,  
591 Skarlou-Alexiou, V., Topcuoğlu, S., Twining, J., Uchida, S., Wasserman, M., 2002.  
592 Generic values for soil-to-plant transfer factors of radiocesium. *J. Environ. Radioact.* 58,  
593 113–128.

594 IAEA-TECDOC-472, 2010. Handbook of parameter values for the prediction of radionuclide  
595 transfer in terrestrial and freshwater. Vienna.

596 Lasat, M.M., Norvell, W.A., Kochian, L. V, 1997. Potential for phytoextraction of<sup>137</sup>Cs  
597 from a contaminated soil. *Plant Soil* 195, 1997.

598 Mück, K., 2003. Sustainability of radiologically contaminated territories. *J. Environ.*  
599 *Radioact.* 65, 109–130. [https://doi.org/10.1016/S0265-931X\(02\)00091-7](https://doi.org/10.1016/S0265-931X(02)00091-7)

600 Noordijk, H., Van Bergeijk, K.E., Lembrechts, J., Frissel, M.J., 1992. Impact of ageing and  
601 weather conditions on soil-to-plant transfer of radiocesium and radiostrontium. *J.*  
602 *Environ. Radioact.* 15, 277–286.

603 Renaud, R., Louvat, D., 2004. Magnitude of fission product depositions from atmospheric  
604 nuclear weapon test fallout in France. *Health Phys.* 86, 353–8.  
605 <https://doi.org/10.1097/00004032-200404000-00003>

606 Rosén, K., Öborn, I., Lönsjö, H., 1999. Migration of radiocaesium in Swedish soil profiles  
607 after the Chernobyl accident, 1987–1995. *J. Environ. Radioact.* 46, 45–66.

608 Roussel-Debet, S., Colle, C., 2005. Comartement de radionucléides (Cs, I, Sr, Se, Tc) dans le  
609 sol: proposition de valeurs de Kd par défaut. *Radioprotection* 40, 203–229.

610 Roussel-Debet, S., Renaud, P., Métivier, J., 2007. <sup>137</sup>Cs in French soils : Deposition patterns  
611 and 15-year evolution. *Sci. Total Environ.* 374, 388–398.  
612 <https://doi.org/10.1016/j.scitotenv.2006.12.037>

613 Smith, J.T., Fesenko, S. V., Howard, B.J., Horrill, A.D., Sanzharova, N.I., Alexakhin, R.M.,  
614 Elder, D.G., Naylor, C., 1999. Temporal change in fallout <sup>137</sup>Cs in terrestrial and  
615 aquatic systems : A whole ecosystem approach. *Environ. Sci. Technol.* 33, 49–54.

616 <https://doi.org/10.1021/es980670t>

617 Smolders, E., Van Den Brande, K., Merckx, R., 1997. Concentrations of <sup>137</sup>Cs and K in soil  
618 solution plant availability of <sup>137</sup>Cs in soils. *Environ. Sci. Technol.* 31, 3432–3438.  
619 <https://doi.org/10.1021/es970113r>

620 Tarsitano, D., Young, S.D., Crout, N.M.J., 2011. Evaluating and reducing a model of  
621 radiocaesium soil-plant uptake. *J. Environ. Radioact.* 102, 262–269.  
622 <https://doi.org/10.1016/j.jenvrad.2010.11.017>

623 Uematsu, S., Smolders, E., Sweeck, L., Wannijn, J., Hees, M. Van, Vandenhove, H., 2015.  
624 Predicting radiocaesium sorption characteristics with soil chemical properties for  
625 Japanese soils. *Sci. Total Environ.* 524–525, 148–156.  
626 <https://doi.org/10.1016/j.scitotenv.2015.04.028>

627 Vrugt, J.A., 2016. Markov chain Monte Carlo simulation using the DREAM software  
628 package: Theory, concepts, and MATLAB implementation. *Environ. Model. Softw.* 75,  
629 273–316. <https://doi.org/10.1016/j.envsoft.2015.08.013>

630 Wright, S.M., Smith, J.T., Beresford, N.A., Scott, W.A., 2003. Monte-Carlo prediction of  
631 changes in areas of west Cumbria requiring restrictions on sheep following the  
632 Chernobyl accident. *Radiat. Environ. Biophys.* 42, 41–47.

633 Yamamura, K., Fujimura, S., Ota, T., Ishikawa, T., Saito, T., Arai, Y., Shinano, T., 2018. A  
634 statistical model for estimating the radiocesium transfer factor from soil to brown rice  
635 using the soil exchangeable potassium content. *J. Environ. Radioact.* 195, 114–125.

636